1521-009X/47/8/802–808$35.00
DRUG METABOLISM AND DISPOSITION

https://doi.org/10.1124/dmd.119.086579
Drug Metab Dispos 47:802–808, August 2019

Short Communication

Kidney Cortical Transporter Expression across Species Using Quantitative Proteomics[S]

Received January 25, 2019; accepted May 20, 2019

ABSTRACT

Limited understanding of species differences in kidney transporters is a critical knowledge gap for prediction of drug-induced acute kidney injury, drug interaction, and pharmacokinetics in humans. Here, we report protein abundance data of 19 transporters in the kidney cortex across five species (human, monkey, dog, rat, and mouse). In general, the abundance of all of the 19 membrane transporters was higher in preclinical species compared with human except for multidrug resistance protein 1 (MDR1), organic cation transporter (OCT) 3, and OCTN1. In nonhuman primate, the total abundance of 12 transporters for which absolute data were available was 2.1-fold higher ($P = 0.025$) relative to human but the percentage of distribution of these transporters was identical in both species. Multidrug resistance-associated protein (MRP) 4, OCTN2, organic anion transporter (OAT) 2, sodium/potassium-transporting ATPase, MRP3, SGLT2, OAT1, MRP1, MDR1, and OCT2 were expressed differently with cross-species variabilities of 8.2-, 7.4-, 6.1-, 5.9-, 5.4-, 5.2-, 4.1-, 3.3-, and 2.8-fold, respectively. Sex differences were only significant in rodents and dog. High protein-protein correlation was observed in OAT1 versus MRP2/MRP4 as well as OCT2 versus MATE1 in human and monkey. The cross-species and sex-dependent protein abundance data are important for animal to human scaling of drug clearance as well as for mechanistic understanding of kidney physiology and derisking of kidney toxicity for new therapeutic candidates in drug development.

Introduction

In the early toxicity assessment of candidate therapeutics in drug development, the data obtained from animal models need to be interpreted with caution for predicting human pharmacokinetics (PK) (Tang and Mayersohn, 2011) and risk of organ injury as well as drug-drug interactions (Fisel et al., 2014). Clinical and preclinical species differences in the mRNA expression, protein abundance, and activity of transporters in organs relevant to drug disposition (i.e., intestine, liver, and kidney) remain a major reason for the poor allometric scaling (Wang et al., 2015). Although significant progress has been made toward the understanding of species and sex differences of drug transporters in the liver (Wang et al., 2015), limited data exist in the kidney and intestine. Particularly, kidney transporters can affect systemic drug clearance by regulating drug secretion and/or reabsorption and contribute to kidney toxicity by affecting intracellular drug concentration (Filipski et al., 2009). For example, kidney toxicity of tenofovir, methotrexate, cisplatin, ifosfamide, ciprofloxacin, and sitagliptin is associated with solute carrier transporters such as organic anion transporters (OATs) and organic cation transporters (OCTs) (Fisel et al., 2014) (Fig. 1). Allometric scaling methods are used for extrapolation of preclinical renal disposition data to human (Zou et al., 2012); however, these methods are not always successful, particularly when a drug undergoes kidney transport and metabolism. For example, tenofovir is taken up into proximal tubules mainly by OAT1 and effluxed into the urine by multidrug resistance-associated protein (MRP) 4, and both of these transporters are shown to be associated with tenofovir kidney toxicity (Kohler et al., 2011). Furthermore, examples exist where kidney toxicity is different in males and females, e.g., cisplatin, an OCT2 substrate, is more toxic to male rats (Nematbakhsh et al., 2013). In addition, rise in serum creatinine (sCr) is used as a surrogate of kidney function. However, since a fraction of sCr is secreted by active transporters, cross-species and sex-dependent variability in sCr transport could lead to false positive or negative conclusions regarding kidney function. In particular, a rise in sCr could be a result of inhibition of renal transporters without direct kidney injury (Chu et al., 2016).

Therefore, characterization of the cross-species and sex-dependent differences in protein abundances of kidney transporters is important for scaling and better prediction of renal secretion, reabsorption, and toxicity in humans. Accordingly, we hypothesized that mapping interspecies and sex differences in the abundance of kidney cortical transporters would enable development of physiologically based PK (PBPK) models that will improve the prediction of PK, kidney toxicity, and the potential risk of drug-drug interactions.

Materials and Methods

Chemicals and Reagents. Liquid chromatography mass spectrometry (MS) grade acetonitrile, methanol, chloroform, and formic acid were purchased from Fisher Scientific (Fair Lawn, NJ) and formic acid was purchased from Sigma-Aldrich (St. Louis, MO). The ProteoExtract native membrane protein extraction kit was procured from Pierce Biotechnology (Rockford, IL). The protein quantification bicinchoninic acid kit and in-solution trypsin digestion kit were purchased from Pierce Biotechnology. Iodoacetamide, dithiothreitol, and pierce trypsin protease (MS grade) were purchased from Thermo Fisher

This project was supported and funded by Pfizer Inc.
Z.R. and V.S.V. are employed by Pfizer Inc.
https://doi.org/10.1124/dmd.119.086579.
[S]This article has supplemental material available at dmd.aspetjournals.org.

ABBREVIATIONS: CL, clearance; LC-MS/MS, liquid chromatography–tandem mass spectrometry; MDR1, multidrug resistance protein 1; MRP, multidrug resistance-associated protein; MS, mass spectrometry; OAT, organic anion transporter; OCT, organic cation transporter; PBPK, physiologically based pharmacokinetics; PK, pharmacokinetics; sCr, serum creatinine.

Scientific (Rockford, IL). Ammonium bicarbonate buffer (98% purity) was purchased from Acros Organics (Geel, Belgium). Human serum albumin and bovine serum albumin were obtained from Calbiochem (Billerica, MA) and Thermo Fisher Scientific, respectively. Surrogate light and heavy peptides were obtained from New England Peptides (Boston, MA) and Thermo Fisher Scientific, respectively. OAT1 antibody was procured from Abcam (Cambridge, MA), anti-mouse IgG horseradish peroxidase–linked secondary antibody was purchased from (Cell Signaling Technologies) and SDS gel (Mini-PROTEAN TGX) was obtained from Bio-Rad (Hercules, CA).

Procurement of Normal Kidney Cortices from Experimental Animals. Normal kidney cortical tissue (approximately 100–150 mg) was collected consistently at autopsy from the same kidney region from the preclinical species, i.e., cynomolgus monkey ($n = 11$; five males and six females), beagle dog ($n = 12$; six males and six females), Wistar Han rat ($n = 20$; 10 males and 10 females), and CD-1 mouse ($n = 18$; eight males and 10 females). The autopsies were conducted at the Pfizer Worldwide R&D facility (Cambridge, MA), which is accredited by the Association for Assessment and Accreditation of Laboratory Animal Care International. After collection, kidney tissue was flash frozen and stored at −80°C before shipping to the University of Washington. The study was conducted in accordance with the National Research Council Guide for the Care and Use of Laboratory Animals (https://grants.nih.gov/grants/olaw/Guide-for-the-Care-and-use-of-laboratory-animals.pdf) and in compliance with the Animal Welfare Act and its implementing regulations, under Institutional Animal Care and Use Committee approved protocols.

Membrane Protein Isolation from Kidney Tissue. Total membrane protein was extracted from the kidney cortex (~30–60 mg) of preclinical species using a previously described protocol (Xu et al., 2018). In brief, 30–60 mg of kidney cortical tissue was homogenized using a handheld rotary homogenizer with plastic probes. The homogenate was centrifuged at 16,000*g* for 30 minutes at 4°C. The supernatant (cytosolic fraction) was transferred to a new tube and the remaining pellet (membrane fraction) was resuspended with 600 μl of solubilization buffer (Pierce Biotechnology) and incubated at 4°C for 30 minutes with continuous mixing. The membrane fraction was used for transporter quantification.

Peptide Selection and Liquid Chromatography–Tandem Mass Spectrometry Protein Quantification of Kidney Drug Transporters. We applied an optimized liquid chromatography–tandem mass spectrometry (LC-MS/MS) methodology, which relies on selective quantification of surrogate peptides of drug transporters. Whenever applicable, conserved peptides across species were selected for precise comparison. When conserved peptides were not available, a novel matrix approach (Supplemental Fig. 1) was used.

Peptide selection for individual drug transporters (Supplemental Table 1) in kidney across species was performed using a previously discussed in silico approach (Bhatt and Prasad, 2018). Total protein in kidney samples was quantified using a bicinchoninic acid assay kit (Pierce Biotechnology) following the vendor protocol. Samples were digested as described previously (Bhatt et al., 2019). Briefly, 80 μl of the membrane sample (2 mg/ml total protein) was mixed with 30 μl ammonium bicarbonate buffer (100 mM), 10 μl of human serum albumin (10 mg/ml), and 20 μl of bovine serum albumin (0.02 mg/ml) in a 1.5 ml microcentrifuge tube. Proteins were denatured and reduced with 10 μl of 250 mM dithiothreitol at 95°C for 10 minutes with gentle shaking at 300 rpm. The sample was cooled at room temperature for 10 minutes, and the denatured protein was alkylated with 20 μl of 500 mM iodoacetamide; the reaction was carried out in the dark for 30 minutes. Ice-cold methanol-chloroform (600 μl, 5:1 v/v) and water (400 μl) were subsequently added to each sample. After vortex mixing and centrifugation at 16,000*g* (4°C) for 5 minutes, the upper aqueous and lower organic layers were carefully removed without disturbing the protein pellet by using vacuum suction. The protein pellet was dried at room temperature for 10 minutes and then washed with 500 μl ice-cold methanol, followed by centrifugation at 8000*g* (4°C) for 5 minutes. The supernatant was removed and the pellet was dried at room temperature for 30 minutes and resuspended in 60 μl of ammonium bicarbonate buffer (50 mM, pH 7.8). Finally, the reconstituted protein sample was digested by adding 20 μl of trypsin (the protein:trypsin ratio was approximately 50:1) and incubated at 37°C for 16 hours. The reaction was quenched by the addition of 20 μl of peptide internal standard cocktail (prepared in 80% acetonitrile in water containing 0.5% formic acid) and 10 μl 80% acetonitrile in water containing 0.5% formic acid. The sample was mixed by vortex mixing and centrifuged at 4000*g* for 5 minutes. The supernatant was collected in a liquid chromatography MS vial for analysis. LC-MS/MS data acquisition was performed on a Waters Acquity UPLC system coupled with a SCIEX API-6500 triple quadrupole mass spectrometer using the optimized parameters outlined in Supplemental Tables 2 and 3 as per the validated method described previously (Prasad et al., 2016). LC-MS/MS data analysis is discussed in the Supplemental Material. Previously published human transporter levels were used as the reference data (Prasad et al., 2016), whereas an archived pooled ($n = 21$) human kidney tissue sample from our previous study was analyzed along with the animal samples as a quality control.

To control for cross-species variability in the membrane isolation recovery, we used total membrane protein per gram of kidney, which served as a scaling factor to express data in picomoles per gram unit. This scaling was particularly important since the total membrane protein per gram of kidney value for human (Supplemental Fig. 2) was significantly lower among species. To validate the LC-MS/MS results, western blotting analysis of a representative protein, OAT1, was performed using an established protocol (Neradugomma et al., 2017) (Supplemental Material).

Results

Cross-Species Kidney Cortical Transporter Abundances. We quantified and investigated 19 basolateral and apical membrane transporters in normal kidney cortices obtained from four commonly used preclinical species in toxicity studies and drug safety evaluation and development, i.e., nonhuman primates (cynomolgus monkeys), beagle dogs, Wistar Han rats, and CD-1 mice. These data were compared with our previously generated human kidney data (Prasad et al., 2016). We report absolute data for 12 transporters (picomoles per gram of tissue) and relative abundance (normalized to total protein) data for seven transporters (Fig. 2; Supplemental Table 4). In general, the abundance of all of the 19 membrane transporters was higher in preclinical species compared with human except for multidrug resistance protein 1 (MDR1), OCT3, and OCTN1 (Fig. 2B). Human MDR1 abundance was similar to monkey, dog, and rat but it was 2.5-fold higher than mouse MDR1 ($P < 0.05$). OCT3 was only detectable in human and OCTN1 was similar in human and monkey. In nonhuman primate, the total abundance of 12 transporters for which absolute data were available was 2.1-fold higher ($P = 0.025$) relative to human but the percentage of distribution of these transporters was identical in both species (Supplemental Fig. 3). The abundance of OAT1, OCTN2, SGLT2, MRP1, sodium/potassium-transporting ATPase, and MRP3 was highest in rat and lowest in human with a fold range of 2.9–7.4 ($P < 0.05$). MRP4 was highest in nonhuman primate and lowest in mouse. The abundance of OAT2 was ~5-fold ($P < 0.0001$) higher in mouse compared with human and nonhuman primate and was undetectable in rat. MATE1, MRP2, OAT3, OAT4, and OATP4C1 were 1.5- to 2.3-fold ($P < 0.05$) higher in nonhuman primate than human. OCT1 and breast cancer resistance protein were only detected in rodents. SGLT2 and sodium/potassium-transporting ATPase were 2- to 6-fold higher in all four preclinical species than human ($P < 0.05$). A significant correlation was observed between transporters (Fig. 3).

Sex Differences in Kidney Cortical Transporter Abundances. Transporter abundance in human and nonhuman primate kidney did not show a sex-dependent pattern. Significant sex differences in transporter abundance were observed in mouse followed by rat > dog (Table 1). OAT1 was higher by 3.2- and 1.3-fold ($P < 0.05$) in male mouse and rat, respectively. OAT2 was 1.6-fold higher in male mouse than female. OCT2 was higher in male rat and mouse. MDR1 was 2- and 1.4-fold higher ($P < 0.05$) in female in mouse and dog, respectively, whereas MDR1 abundance was higher in male rat by 1.6-fold. MRP4 is predominantly expressed in male mouse (2.4-fold,

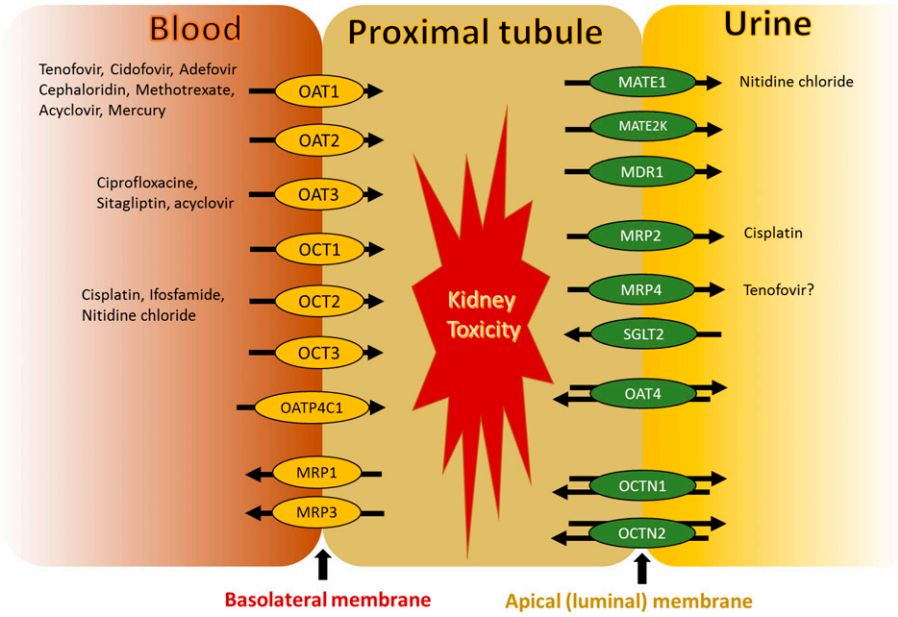

Fig. 1. Localization of drug transporters in proximal tubule. Kidney proximal tubule contains OAT1-3, OATP4C1, OCT1-3, and MRP1/3 at the basolateral membrane and MATE1, MATE2k, MDR1, MRP2/4, SGLT2, OAT4, and OCTN1/2 at the apical membrane. Both uptake and efflux drug transporters are involved in nephrotoxicity of certain drugs shown in the figure.

$P < 0.05$) kidney. OCTN2 abundance was 1.3- and 1.4-fold higher in female mouse and male rats, respectively. SGLT2 was only 1.2-fold higher ($P < 0.05$) in female rats.

Comparison of LC-MS/MS Proteomics and Western Blot Data of Representative Transporter OAT1. Antibodies are not available for all the studied transporters and when available, these do not work for all species. Nevertheless, we performed OAT1 quantification by western blotting using an anti-mouse OAT1 antibody to validate the LC-MS/MS data (the method is discussed in the Supplemental Material). The sex difference in OAT1 abundance in mouse was qualitatively confirmed by the western blot data (Supplemental Fig. 4). The higher signal of OAT1 in the rat sample was consistent with the proteomics data; however, the antibody did not work for human OAT1 (data not shown).

Discussion

Here, we report a comparison of 19 clinically relevant kidney drug transporters between human and four common preclinical animal models used in drug development. The presented data are the total membrane expression because it is technically difficult to reproducibly extract purified plasma membrane from frozen tissues (Kumar et al., 2015). While plasma membrane isolation involves multiple steps, we have previously demonstrated that total membrane extraction from different parts of the kidney is highly reproducible using the total membrane extraction kit (Prasad et al., 2016).

The quantitative information on cross-species transporter abundance is useful in interpreting kidney safety data in humans. In particular, drug-induced modest rises (20%–30%) in sCr in preclinical models could be due to direct tubular damage (i.e., drug-induced kidney injury) or indirect inhibition of kidney transporters. For example, an investigational Janus kinase inhibitor, INCB039110 (itacitinib), resulted in rises in sCr in a healthy volunteer's study (Zhang et al., 2015). A follow-up dedicated kidney investigative clinical study revealed no changes in Food and Drug Administration/European Medicines Agency qualified nonclinical kidney toxicity biomarkers (e.g., Cystatin C) or glomerular filtration rate, but rather the rises in sCr were attributed to interference with kidney uptake transporters such as OCT2, OCT3, and OAT2 (Zhang et al., 2015) and efflux transporters such as MATE1 and MATE2K (Lepist et al., 2014; Zhang et al., 2015). Thus, understanding which transporters are potentially involved in uptake or efflux of the therapeutic candidate and knowing the relative abundance of the transporter across nonclinical species and humans will allow better interpretation of clinical data.

This data set for species and sex-specific abundances for kidney transporters is also useful to the biomedical community and drug developers in predicting the drug clearance and safety of new molecule entities. In agreement with our data, OCT1 and breast cancer resistance protein were not detected in human and nonhuman primate but were abundant in rodents (Bleasby et al., 2006; Prasad et al., 2016). The relatively low abundance of MDR1 in mouse kidney compared with human and rat is consistent with the mRNA data (Bleasby et al., 2006). Similarly, both nonhuman primate and rat have been shown to be associated with kidney toxicity with repeated dosing of tenofovir; however, such toxicity was not observed in the mouse at a similar dose (Ng et al., 2015; Ustianowski and Arends, 2015). The high correlation between OAT1 versus MRP2 and MRP4 indicates that the latter are important for the apical efflux of organic anions. Similarly, the high correlation of cation transporters OCT2 and MATE1 in human and nonhuman primate perhaps suggests that these transporters are coregulated. We also observed that OAT2 (a sCr secreting transporter) is a highly abundant anion transporter in mouse, whereas OAT1 is predominantly expressed in other species. Therefore, results of individual OAT knockout mouse versus rat are expected to be significantly different.

Differential sex abundance in mouse and rat (Table 1) was supported by negative correlations between transporters (Fig. 3). In particular, in the mouse the basolateral uptake transporters such as OATs and OCT2 were higher in male but the apical transporters (primarily efflux) were higher in females. In the rat, sex-dependent regulation of the basolateral uptake transporters was consistent with mouse; however, OCTN2, breast cancer resistance protein, and P-glycoprotein were also higher in males. Although the mechanisms of sex-dependent expression of these proteins are unknown, these transporters are important in secretion of conjugated sex hormones (Bush et al., 2017), and therefore can be regulated by the latter.

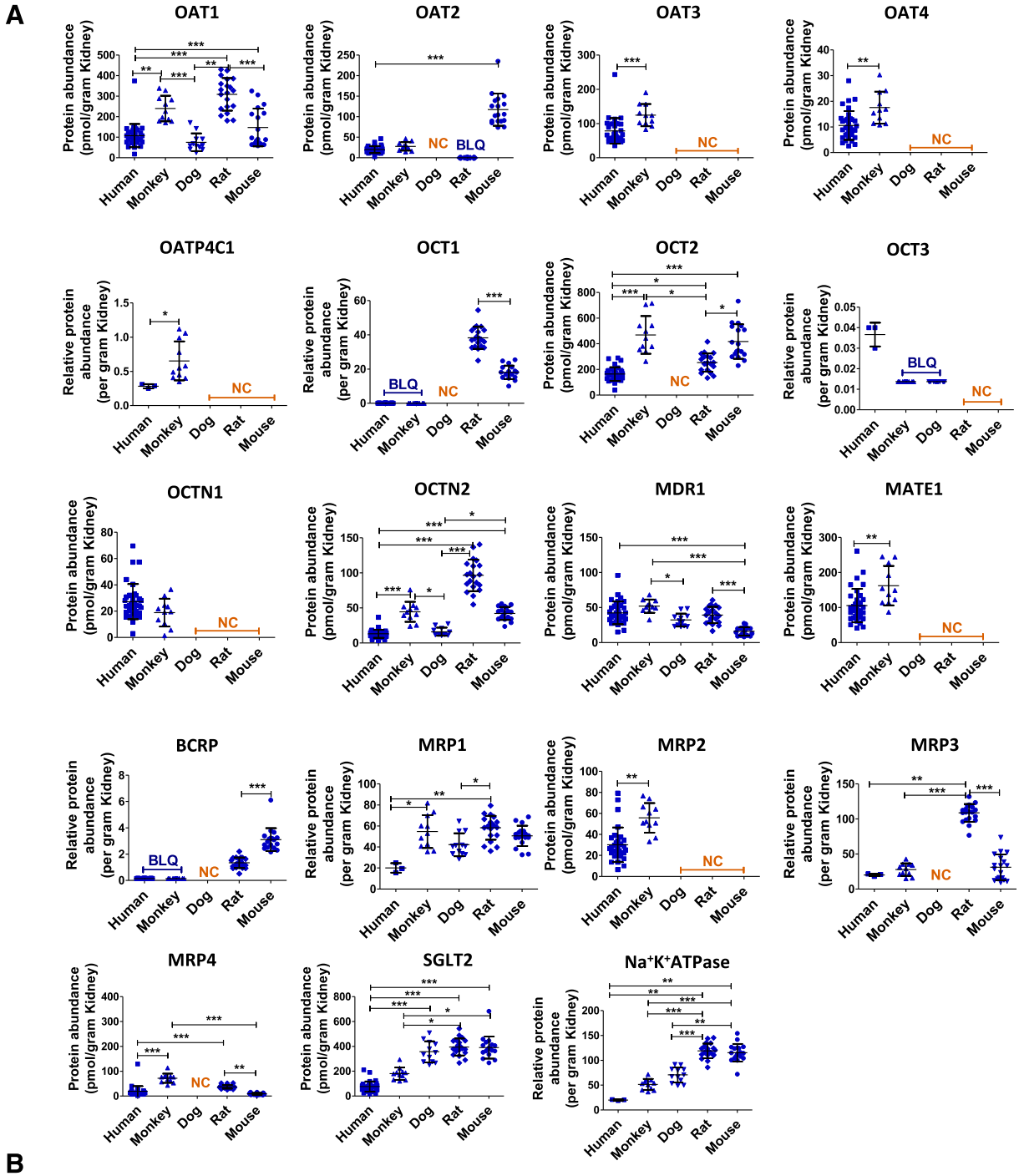

B

Species	Transporters (Proteins)																		
	OAT1	OAT2	OAT3	OAT4	OATP4C1	OCT1	OCT2	OCT3	OCTN1	OCTN2	MDR1A	MATE1	BCRP	MRP1	MRP2	MRP3	MRP4	SGLT2	Na+K+ATPase
Human	1.0	1.0	1.0	1.0	1.0	BLQ	1.0	Detectable	1.0	1.0	1.0	1.0	BLQ	1.0	1.0	1.0	1.0	1.0	1.0
Monkey	2.3	1.4	1.6	1.7	2.3	BLQ	2.8	BLQ	0.7	3.4	1.2	1.5	BLQ	2.7	1.9	1.4	3.7	2.4	2.6
Dog	0.7	NC	NC	NC	NC	NC	NC	BLQ	NC	1.2	0.8	NC	NC	2.1	NC	NC	NC	4.7	3.5
Rat	2.9	BLQ	NC	NC	NC	1.0	1.5	NC	NC	7.4	0.9	NC	1.0	2.9	NC	5.4	1.9	5.2	5.9
Mouse	1.5	6.1	NC	NC	NC	0.5	2.6	NC	NC	3.2	0.4	NC	2.3	2.5	NC	1.5	0.4	5.1	5.7

High
Low

Fig. 2. (A) Kidney cortical transporter cross-species comparison of protein abundance (picomoles per gram tissue) expression. Each dot represents the individual sample and data are represented as mean ± S.D. MATE2K was not detectable in any species because of poor sensitivity of the surrogate peptide. Only six transporters were detected in dog kidney because of the lack of conserved peptides. (B) Heat map of relative quantitative abundance of kidney transporters across species. Value in the cell represents the relative abundance of transporters across different species compared with transporter abundance in human kidney. Yellow to red color indicates increasing abundance of a particular transporter across species.

Consistent with our data, the abundance and activity of some OATs and OCTs have been shown to be sex dependent (Cerrutti et al., 2002; Groves et al., 2006; Breljak et al., 2010; da Silva Faria et al., 2015).

Good correlation of OAT1 and OAT3 abundance is supported by the fact that these are transcriptionally coregulated (Prasad et al., 2016). Because most of the coregulated proteins work in tandem

A

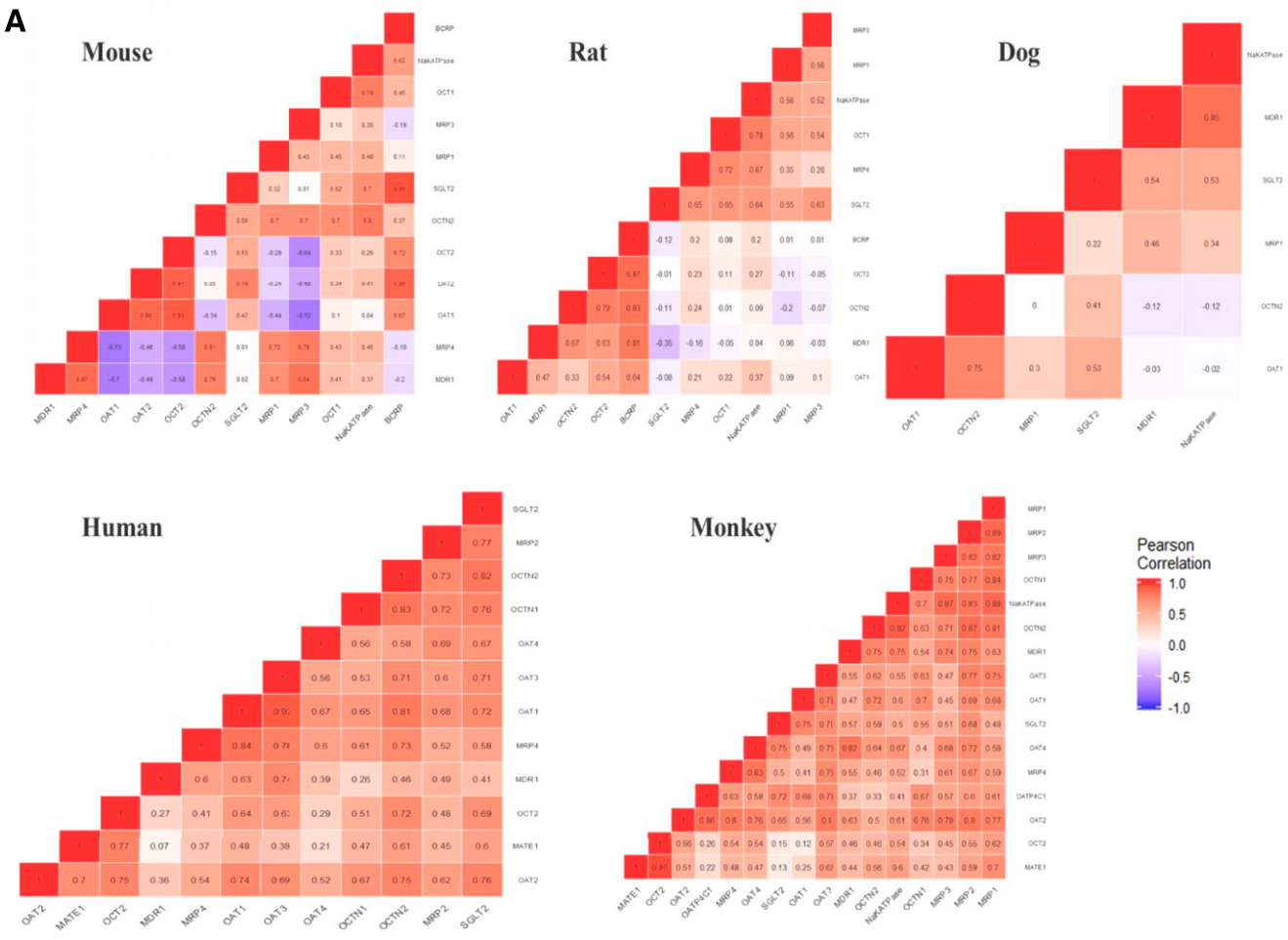

B

Species	Transporters (Proteins)																		
		OAT1	OAT2	OAT3	OAT4	OATP4C1	OCT1	OCT2	OCT3	OCTN1	OCTN2	MDR1A	MATE1	BCRP	MRP1	MRP2	MRP3	MRP4	SGLT2	Na+K+ATPase
	Human	MRP2, MRP4, OAT3, OCTN2	MATE1, OCT2, OCTN2, SGLT2	MRP4, OAT1	NS	NS	BLQ	OAT2, MATE1	Detected	OCTN2, SGLT2	OAT1-2, SGLT2	NS	OAT2, OCT2	BLQ	NS	SGLT2, OAT1	NS	OAT1, OAT3	OAT2, OCTN1-2, MRP2	NS
	Monkey	SGLT2, OAT3	OATP4C1, MRP1-4, OAT3-4, OCTN1	OAT1, OAT2, MRP1, MRP2	MRP4, SGLT2, OAT2, MDR1	OAT2,	BLQ	MATE1,	BLQ	MRP1-3, OAT2	MDR1, MRP1-2 Na+K+ATPase	OCT2, OCTN2, OAT4, MRP2, Na+K+ATPase	NS	BLQ	MRP2-3, OCTN1-2, OAT2-3 Na+K+ATPase	MRP1, OCTN1, OAT2-3 OCTN2, MDR1, Na+K+ATPase	OCTN1, MRP1, OAT2, Na+K+ATPase	OAT2, OAT4	OAT1, OAT4	OCTN2, MRP1-3 MDR1
	Dog	OCTN2	NC	NC	NC	NC	NC	NC	BLQ	NC	OAT1	NS	NS	NS	NS	NC	NC	NC	NS	MDR1
	Rat	NS	BLQ	NC	NC	NC	Na+K+ATPase	OCTN2, BCRP	NC	NC	OCT2, BCRP	BCRP,	NS	OCT2, OCTN2, MDR1	NS	NC	NS	NS	NS	OCT1,
	Mouse	OCT2, OAT2	OAT1, OCT2, SGLT2, BCRP	NS	NC	NC	Na+K+ATPase	OAT1	NC	NC	MRP4, MDR1	OCTN2, MRP3	NS	SGLT2, OAT2	NS	NC	MRP4, MDR1	OCTN2, MRP3	OAT2, BCRP	OCT1, OCTN2

Fig. 3. (A) Correlation plot for kidney transporter proteins across all five species. Values in the cell represent the coefficient of correlation (r^2) between two transporter proteins. (B) Positive correlation between the transporter proteins with $r^2 > 0.70$. The number of samples from individual species used in this study (with few exceptions) was human ($n = 34$), monkey ($n = 11$), dog ($n = 12$), rat ($n = 20$), and mouse ($n = 18$). Not conserved (NC) indicates that a conserved peptide was not found for that particular species. BLQ denotes below limit of quantification but the peptide was conserved. The BLQ values were derived by extrapolation of the signal-to-noise ratio to 3. No significant (NS) correlation ($r^2 < 0.70$) was found between transporter proteins.

(OCT vs. multidrug and toxin extrusion protein and OAT vs. MRP) in the vectorial transport process, substrate-mediated regulation could be tested as a potential mechanism of correlations.

Regarding the limitations of this study, it does not allow comparison of all transporters because of the lack of MS-quantifiable or conserved peptides across species (e.g., dog). Nevertheless, our novel LC-MS/MS proteomics method allowed quantification of a majority of kidney transporters across species, which is not currently feasible using conventional immunoquantification. We also demonstrated that the quality of the LC-MS/MS proteomics data is superior to western blot data using OAT1 as an example (Supplemental Fig. 4). In addition, the protein abundance data (in the absence of in vitro functional data) are limited for the prediction of species differences in drug-induced kidney injury or PK. However, the transporter abundance data are a critical piece of information (i.e., a prerequisite), which constitute key physiologic parameters for PBPK modeling (Harwood et al., 2013). In particular, these data can be integrated with transport kinetics data (e.g., K_m in eq. 1) of a drug or new chemical entity to

TABLE 1

Sex differences in protein abundance of transporters across species

Protein	Human	Monkey	Dog	Rat	Mouse
SLC22A6/OAT1	↔	↔	↔	M > F *1.3	M > F *3.2
SLC22A7/OAT2	↔	↔	NC	BLQ	M > F *1.6
SLC22A8/OAT3	↔	↔	NC	NC	NC
SLC22A11/OAT4	↔	↔	NC	NC	NC
SLCO4C1/OATP4C1	ND	↔	NC	NC	NC
SLC22A1/OCT1	BLQ	BLQ	NC	↔	↔
SLC22A2/OCT2	↔	↔	NC	M > F *1.4	M > F *1.6
SLC22A4/OCTN1	↔	↔	NC	NC	NC
SLC22A5/OCTN2	↔	↔	NC	M > F *1.4	F > M *1.3
ABCB1/MDR1	↔	↔	F > M *1.4	M > F *1.6	F > M *2.0
SLC47A1/MATE1	↔	↔	NC	NC	NC
ABCG2/BCRP	BLQ	BLQ	NC	M > F *1.6	↔
ABCC1/MRP1	ND	↔	↔	↔	F > M *1.3
ABCC2/MRP2	↔	↔	NC	NC	NC
ABCC3/MRP3	ND	↔	NC	F > M *1.1	F > M *3.1
ABCC4/MRP4	↔	↔	NC	↔	F > M *2.4
SLC5A2/SGLT2	↔	↔	↔	F > M *1.2	↔
ATP1A1/Na^+/K^+-ATPase	ND	↔	F > M *1.3	↔	↔

ABCB, ATP-binding cassette subfamily B; ABCC, ATP-binding cassette subfamily C; ABCG, ATP-binding cassette superfamily G; BCRP, breast cancer resistance protein; BLQ, below limit of quantification; F, female; M, male; NC, peptide not conserved; Na^+/K^+-ATPase, sodium/potassium-transporting ATPase; ND, sex difference was not determined, data were obtained with pooled quality control samples; ↔, no significant difference; *, fold difference.

predict in vivo transporter activity in animal versus human models (eq. 2). Furthermore, sex-dependent quantitative differences in the transporter abundance can be directly integrated into a PBPK model to extrapolate drug PK or drug toxicity (eqs. 1 and 3); where K_m can be assumed similar between male versus female in a single species:

$$CL = \frac{V_{max}}{K_m + [S]} = \frac{[\text{Abundance} \times K_{cat}]}{K_m + [S]} \quad (1)$$

Thus,

$$CL_{human}\ \alpha CL_{animal} \times \frac{[\text{Abundance}_{human}]}{[\text{Abundance}_{animal}]} \quad (2)$$

$$CL_{female} = CL_{male} \times \frac{[\text{Abundance}_{human}]}{[\text{Abundance}_{animal}]} \quad (3)$$

where CL is the intrinsic clearance (picomoles per minute per milligram protein or picomoles per minute per gram of kidney); V_{max} is the maximum transport activity; K_m is substrate affinity to a transporter; K_{cat} is the turnover number; and [S] is the substrate concentration. Here, V_{max} depends on the transporter abundance, whereas K_m and K_{cat} are independent of protein levels (Bhatt and Prasad, 2018). It is also noteworthy that the data obtained from the absolute peptide approach should not be considered as absolute molar protein abundance data because complete trypsin digestion may not be confirmed. However, these data (absolute peptide levels) can be used in allometric scaling of animal-to-human transporter-mediated clearances using eqs. 1–3. Because the scaling factor is derived by dividing the peptide abundance values, it does not matter whether absolute protein or absolute peptide values are used in the scaling as long as the trypsin digestion and the sample extraction are reproducible and consistent across species/genders. We have previously described this scaling approach (Bhatt and Prasad, 2018).

In summary, our data on cross-species kidney transporter abundances, particularly in human, monkey, and rodents, provide useful quantitative information, which can be leveraged by: 1) allowing for preclinical-to-clinical translation of transporter-mediated secretary clearance using PBPK modeling, 2) distinguishing direct drug-induced kidney toxicity from indirect impact on kidney transporters (e.g., transporter-mediated creatinine clearance), and 3) utilizing cross-species transporter levels in conjunction with kidney injury biomarkers to better understand kidney safety signals and human safety risk assessment.

Acknowledgments

The authors thank Dr. Naveen Neradugomma for help with the western blotting analysis.

Department of Pharmaceutics, University of Washington, Seattle, Washington (A.B., M.K., B.P.); and Pfizer Worldwide Research Development, Drug Safety Research Development, Cambridge, Massachusetts (Z.R., V.S.V.)

Abdul Basit
Zaher Radi
Vishal S. Vaidya
Matthew Karasu
Bhagwat Prasad

Authorship Contributions

Participated in research design: Basit, Radi, Vaidya, Prasad.
Conducted experiments: Basit, Karasu.
Performed data analysis: Basit, Prasad.
Wrote or contributed to the writing of the manuscript: Basit, Radi, Vaidya, Prasad.

References

Bhatt DK, Mehrotra A, Gaedigk A, Chapa R, Basit A, Zhang H, Choudhari P, Boberg M, Pearce RE, Gaedigk R, et al. (2019) Age- and genotype-dependent variability in the protein abundance and activity of six major uridine diphosphate-glucuronosyltransferases in human liver. *Clin Pharmacol Ther* **105**:131–141.

Bhatt DK and Prasad B (2018) Critical issues and optimized practices in quantification of protein abundance level to determine interindividual variability in DMET proteins by LC-MS/MS proteomics. *Clin Pharmacol Ther* **103**:619–630.

Bleasby K, Castle JC, Roberts CJ, Cheng C, Bailey WJ, Sina JF, Kulkarni AV, Hafey MJ, Evers R, Johnson JM, et al. (2006) Expression profiles of 50 xenobiotic transporter genes in humans and pre-clinical species: a resource for investigations into drug disposition. *Xenobiotica* **36**:963–988.

Breljak D, Ljubojevic M, Balen D, Zlender V, Brzica H, Micek V, Kusan M, Anzai N, and Sabolic I (2010) Renal expression of organic anion transporter Oat5 in rats and mice exhibits the female-dominant sex differences. *Histol Histopathol* **25**:1385–1402.

Bush KT, Wu W, Lun C, and Nigam SK (2017) The drug transporter OAT3 (SLC22A8) and endogenous metabolite communication via the gut–liver–kidney axis. *J Biol Chem* **292**: 15789–15803.

Cerrutti JA, Quaglia NB, Brandoni A, and Torres AM (2002) Effects of gender on the pharmacokinetics of drugs secreted by the renal organic anions transport systems in the rat. *Pharmacol Res* **45**:107–112.

Chu X, Bleasby K, Chan GH, Nunes I, and Evers R (2016) Transporters affecting biochemical test results: creatinine-drug interactions. *Clin Pharmacol Ther* **100**:437–440.
da Silva Faria MC, Santos NA, Carvalho Rodrigues MA, Rodrigues JL, Barbosa Junior F, and Santos AC (2015) Effect of diabetes on biodistribution, nephrotoxicity and antitumor activity of cisplatin in mice. *Chem Biol Interact* **229**:119–131.
Filipski KK, Mathijssen RH, Mikkelsen TS, Schinkel AH, and Sparreboom A (2009) Contribution of organic cation transporter 2 (OCT2) to cisplatin-induced nephrotoxicity. *Clin Pharmacol Ther* **86**:396–402.
Fisel P, Renner O, Nies AT, Schwab M, and Schaeffeler E (2014) Solute carrier transporter and drug-related nephrotoxicity: the impact of proximal tubule cell models for preclinical research. *Expert Opin Drug Metab Toxicol* **10**:395–408.
Groves CE, Suhre WB, Cherrington NJ, and Wright SH (2006) Sex differences in the mRNA, protein, and functional expression of organic anion transporter (Oat) 1, Oat3, and organic cation transporter (Oct) 2 in rabbit renal proximal tubules. *J Pharmacol Exp Ther* **316**: 743–752.
Harwood MD, Neuhoff S, Carlson GL, Warhurst G, and Rostami-Hodjegan A (2013) Absolute abundance and function of intestinal drug transporters: a prerequisite for fully mechanistic in vitro-in vivo extrapolation of oral drug absorption. *Biopharm Drug Dispos* **34**:2–28.
Kohler JJ, Hosseini SH, Green E, Abuin A, Ludaway T, Russ R, Santoianni R, and Lewis W (2011) Tenofovir renal proximal tubular toxicity is regulated by OAT1 and MRP4 transporters. *Lab Invest* **91**:852–858.
Kumar V, Prasad B, Patilea G, Gupta A, Salphati L, Evers R, Hop CE, and Unadkat JD (2015) Quantitative transporter proteomics by liquid chromatography with tandem mass spectrometry: addressing methodologic issues of plasma membrane isolation and expression-activity relationship. *Drug Metab Dispos* **43**:284–288.
Lepist EI, Zhang X, Hao J, Huang J, Kosaka A, Birkus G, Murray BP, Bannister R, Cihlar T, Huang Y, et al. (2014) Contribution of the organic anion transporter OAT2 to the renal active tubular secretion of creatinine and mechanism for serum creatinine elevations caused by cobicistat. *Kidney Int* **86**:350–357.
Nematbakhsh M, Ebrahimian S, Tooyserkani M, Eshraghi-Jazi F, Talebi A, and Ashrafi F (2013) Gender difference in Cisplatin-induced nephrotoxicity in a rat model: greater intensity of damage in male than female. *Nephrourol Mon* **5**:818–821.
Neradugomma NK, Liao MZ, and Mao Q (2017) Buprenorphine, norbuprenorphine, R-methadone, and S-methadone upregulate BCRP/ABCG2 expression by activating aryl hydrocarbon receptor in human placental trophoblasts. *Mol Pharmacol* **91**:237–249.
Ng HH, Stock H, Rausch L, Bunin D, Wang A, Brill S, Gow J, and Mirsalis JC (2015) Tenofovir disoproxil fumarate: toxicity, toxicokinetics, and toxicogenomics analysis after 13 weeks of oral administration in mice. *Int J Toxicol* **34**:4–10.
Prasad B, Johnson K, Billington S, Lee C, Chung GW, Brown CD, Kelly EJ, Himmelfarb J, and Unadkat JD (2016) Abundance of drug transporters in the human kidney cortex as quantified by quantitative targeted proteomics. *Drug Metab Dispos* **44**:1920–1924.
Tang H and Mayersohn M (2011) Controversies in allometric scaling for predicting human drug clearance: an historical problem and reflections on what works and what does not. *Curr Top Med Chem* **11**:340–350.
Ustianowski A and Arends JE (2015) Tenofovir: what we have learnt after 7.5 million person-years of use. *Infect Dis Ther* **4**:145–157.
Wang L, Prasad B, Salphati L, Chu X, Gupta A, Hop CE, Evers R, and Unadkat JD (2015) Interspecies variability in expression of hepatobiliary transporters across human, dog, monkey, and rat as determined by quantitative proteomics. *Drug Metab Dispos* **43**:367–374.
Xu M, Saxena N, Vrana M, Zhang H, Kumar V, Billington S, Khojasteh C, Heyward S, Unadkat JD, and Prasad B (2018) Targeted LC-MS/MS proteomics-based strategy to characterize in vitro models used in drug metabolism and transport studies. *Anal Chem* **90**:11873–11882.
Zhang Y, Warren MS, Zhang X, Diamond S, Williams B, Punwani N, Huang J, Huang Y, and Yeleswaram S (2015) Impact on creatinine renal clearance by the interplay of multiple renal transporters: a case study with INCB039110. *Drug Metab Dispos* **43**:485–489.
Zou P, Yu Y, Zheng N, Yang Y, Paholak HJ, Yu LX, and Sun D (2012) Applications of human pharmacokinetic prediction in first-in-human dose estimation. *AAPS J* **14**:262–281.

Address correspondence to: Dr. Bhagwat Prasad, Department of Pharmaceutics, University of Washington, Seattle, P.O. Box 357610, WA 98195. E-mail: bhagwat@uw.edu

SUPPLEMENTARY INFORMATION

Kidney cortical transporter expression across species using quantitative proteomics

Abdul Basit[1], Zaher Radi[2], Vishal Vaidhya[2], Mathew Karasu[1], Bhagwat Prasad[1]

[1] Department of Pharmaceutics, University of Washington, Seattle, P.O. Box 357610, WA 98195 USA

[2] Pfizer Worldwide Research Development, Drug Safety Research Development, One Portland Street, Cambridge, MA 02139 USA

METHODS

LC-MS/MS Data Analysis

The LC-MS/MS data were analyzed using Skyline 4.1, where the peptide peaks were identified by matching the retention time with heavy internal standards and alignment of selected precursor ion to daughter ion fragments. A previously optimized robust data analysis approach[S4] which considers internal standard protein (BSA), heavy internal standard peptide, and pooled quality control samples was used. In addition, matrix approach was used to estimate transporter protein abundance if a surrogate peptide was not conserved in a particular species (Supplementary Figure 3). The peptide data were initially analyzed as pmol/mg total membrane protein and when more than one peptides were used, the abundance data were presented as the average of peptides. Total membrane protein (mg) per gram kidney tissue (TM-PPGK), was calculated and used for scaling these data to pmol/gram of tissue. The TM-PPGK values for the human ranges from 15.76 to 34.00 mg/g with mean value of 20.1, whereas it was 28.3 ± 5.1, 30.7 ± 7.7, 34.5 ± 4.7, and 28.6 ± 2.0 mg/g for monkey, dog, rat and mouse, respectively (Supplementary Figure 4). Human transporter abundance data were generated previously, which were confirmed using pooled human quality control samples (n=21 previously studied human kidney tissues) in this study. Absolute or relative protein abundance (pmol/g) across species (human, monkey, dog, rat and mouse) was then compared by the Kruskal-Wallis followed by Dunn`s multiple comparison test and Mann-Whitney test. The protein abundance data are presented as mean±SD.

Western Blotting Procedure for OAT1 Quantification

To validate performance of LC-MS/MS data of a representative transporter, OAT1, between male and female mice and across species, Western blotting method, where gel electrophoresis of

membrane fractions (2 mg/mL) of mouse, human and rat kidney cortex was performed using 4-15% SDS gel (Mini-PROTEAN TGX, BIO-RAD). Standard Western blotting protocol was followed (Neradugomma et al., 2017). Briefly, 60 µg of protein from each sample was loaded onto the gel electrophoresis. After protein separation on the gel, proteins were transferred onto immune P-nitrocellulose membrane in transfer buffer (25 mM Tris base, 192 mM Glycin in 20% methanol). The blot was then blocked with 5% dry milk in PBS-T buffer (PBS with 0.1% tween 20) incubating for 1 hr at room temperature (RT). The blot was washed three times with PBS-T and incubated with rabbit polyclonal anti-SLC22A antibody (ab135924, Abcam, Cambridge, MA) at 1:1000 dilution as primary antibody for 1 hr at RT. The blot was washed three times with PBS-T buffer and incubated with anti-mouse IgG, HRP-linked secondary antibody (Cell signaling technologies) at 1:10000 dilution for 1 hr at RT. After washing three times with PBS-T buffer, the blot was developed using a ECL Western Development reagent (GE #RPN2132).

Supplemental Table 1: **List of surrogate peptides for renal transporters across species**. Transporter peptide detected and quantified (green); detected but not quantified (light green); conserved (√); quantified using matrix approach (orange); below limit of quantification (BLQ); and non-conserved peptide (NC).

	Peptide	Human	Monkey	Dog	Rat	Mouse
ABCB1 /MDR1	AGAVAEEVLAAIR LANDAAQVK	√	√	√	√	√
SLC47A1 /MATE1	GGPEATLEVR	√	√	NC	NC	NC
ABCC1 /MRP1	ITIIPQDPVLFSGSLR	√	√	√	√	√
ABCC2 /MRP2	QLLNNILR YFAWEPSFR	√	√	NC	NC	NC
ABCC3 /MRP3	SQLTIIPQDPILFSGTLR	√	√	NC	√	√
	LLEAWQK			NC	√	√
ABCC4 /MRP4	SSLISALFR	√	√	NC	√	√
SLC22A6 /OAT1	LVGFLVINSLGR	√	√	√		
	GQASAMELLR	√	√		√	√
SLC22A7 /OAT2	ACQQAQVHANLK	√	√	NC	√ (BLQ)	√
	NVALLALPR	√	√	NC	NC	
SLC22A8 /OAT3	TVLAVFGK	√	√	NC	NC	NC
SLC22A11 /OAT4	GKPDQALQELR	√	√	NC	NC	NC

SLC22A1 /OCT1	SPSFADLFR	√ (BLQ)	√ (BLQ)	NC	√	√
SLC22A2 /OCT2	WLISQNK	√	√	NC	√	√
	LNPSFLDLVR	√	√	NC	√	√
SLC22A3 /OCT3	GPSAAALAER	√	√ (BLQ)	√ (BLQ)	NC	NC
SLC22A4 /OCTN1	AFILDLFR	√	√	NC	NC	NC
SLC22A5 /OCTN2	WLISQGR	√	√	√	√	√
SLC5A2 /SGLT2	GTVGGYFLAGR	√	√	√	√	√
ABCG2 /BCRP	ENLQFSAALR LFDSLTLLASGK	NC	NC	NC	√	√
ATP1A1/ Na+K+ATPase	IVEIPFNSTNK YHTEIVFAR	√	√	√	√	√

Supplemental Table 2: Chromatographic conditions for separation of surrogate peptides of kidney transporters.

LC gradient program			
ACQUITY UPLC® HSS T3 C18 column (2.1 × 100 mm, 1.8 μm)			
Time (min)	Flow Rate	A (Water with 0.1% formic acid, %)	B (Acetonitrile with 0.1% formic acid, %)
0	0.3	97.0	3.0
4	0.3	97.0	3.0
8	0.3	87.0	13.0
18	0.3	70.0	30.0
20.5	0.3	65.0	35.0
21.1	0.3	40.0	60.0
23.1	0.3	20.0	80.0
23.2	0.3	97.0	3.0
27	0.3	97.0	3.0

Supplemental Table 3: Multiple reaction monitoring (MRM) parameters for analysis of surrogate peptides of kidney transporters. K and R (shown in bold) were labeled as ^{13}C and ^{15}N.

Protein	Peptide	Peptide labeling	Parent Ion	Daughter Ion	DP	CE
ABCB1 /MDR1	AGAVAEEVLAAI**R**	Light	635.4	971.6	77.4	31.7
			635.4	900.5	77.4	31.7
		Heavy	640.4	981.6	77.4	31.7
			640.4	910.5	77.4	31.7
	LANDAAQV**K**	Light	465.3	745.4	65	25.6
			465.3	631.3	65	25.6
		Heavy	469.3	753.4	65	25.6
			469.3	639.4	65	25.6
SLC47A1 /MATE1	HVGVILQ**R**	Light	461.3	685.4	64.7	25.5
			461.3	529.3	64.7	25.5
			461.3	747.5	64.7	25.5
		Heavy	466.3	695.4	64.7	25.5
			466.3	539.4	64.7	25.5
			466.3	747.5	64.7	25.5
	GGPEATLEV**R**	Light	514.8	688.4	68.6	27.4
			514.8	617.4	68.6	27.4
		Heavy	519.8	698.4	68.6	27.4
			519.8	627.4	68.6	27.4
ABCC1 /MRP1	ITIIPQDPVLFSGSL**R**	Light	878.5	1315.7	95.2	40.5
			878.5	658.4	95.2	40.5
			878.5	441.3	95.2	40.5
		Heavy	883.5	1325.7	95.2	40.5
			883.5	663.4	95.2	40.5
			883.5	441.3	95.2	40.5
ABCC2 /MRP2	QLLNNIL**R**	Light	492.3	742.5	67	26.6
			492.3	629.4	67	26.6
		Heavy	497.3	752.5	67	26.6
			497.3	639.4	67	26.6
	YFAWEPSF**R**	Light	601.8	892.4	75	30.5
			601.8	506.3	75	30.5
		Heavy	606.8	902.4	75	30.5
			606.8	516.3	75	30.5
ABCC3 /MRP3	SQLTIIPQDPILFSGTL**R**	Light	1000.1	1343.7	104	44.9
			1000.1	1003.6	104	44.9
			1000.1	656.4	104	44.9
		Heavy	1005.1	1353.7	104	44.9

			1005.1	1013.6	104	44.9
			1005.1	656.4	104	44.9
	LLEAWQ**K**	Light	444.3	661.3	63.5	24.9
			444.3	532.3	63.5	24.9
			444.3	741.4	63.5	24.9
		Heavy	448.3	669.3	63.5	24.9
			448.3	540.3	63.5	24.9
			448.3	741.4	63.5	24.9
ABCC4 /MRP4	SSLISALF**R**	Light	497.3	706.4	67.4	26.8
			497.3	593.3	67.4	26.8
		Heavy	502.3	716.4	67.4	26.8
			502.3	603.3	67.4	26.8
SLC22A6 /OAT1	GQASAMELL**R**	Light	538.3	819.4	70.4	28.2
			538.3	732.4	70.4	28.2
			538.3	661.4	70.4	28.2
		Heavy	543.3	829.4	70.4	28.2
			543.3	742.4	70.4	28.2
			543.3	671.4	70.4	28.2
	LVGFLVINSLG**R**	Light	644.4	758.5	78.1	32.1
			644.4	659.4	78.1	32.1
		Heavy	649.4	768.5	78.1	32.1
			649.4	669.4	78.1	32.1
SLC22A7 /OAT2	AC[CAM]QQAQVHANL**K**	Light	456.6	568.8	64.4	22.4
			456.6	504.8	64.4	22.4
		Heavy	459.2	572.8	64.4	22.4
			459.2	508.8	64.4	22.4
	NVALLALP**R**	Light	483.8	753.5	66.4	26.3
			483.8	569.4	66.4	26.3
		Heavy	488.8	763.5	66.4	26.3
			488.8	579.4	66.4	26.3
SLC22A8 /OAT3	TVLAVFG**K**	Light	417.8	634.4	61.6	23.9
			417.8	521.3	61.6	23.9
		Heavy	421.8	642.4	61.6	23.9
			421.8	529.3	61.6	23.9
SLC22A11 /OAT4	GKPDQALQEL**R**	Light	418.9	658.4	61.7	20.4
			418.9	545.3	61.7	20.4
		Heavy	422.2	668.4	61.7	20.4
			422.2	555.3	61.7	20.4
SLC22A1 /OCT1	SPSFADLF**R**	Light	520.3	768.4	69	27.6
			520.3	621.3	69	27.6

			520.3	476.7	69	27.6
		Heavy	525.3	778.4	69	27.6
			525.3	631.3	69	27.6
			525.3	481.8	69	27.6
SLC22A2 /OCT2	WLISQN**K**	Light	444.8	702.4	63.5	24.9
			444.8	589.3	63.5	24.9
		Heavy	448.8	710.4	63.5	24.9
			448.8	597.3	63.5	24.9
	LNPSFLDLV**R**	Light	587.3	946.5	73.9	30
			587.3	473.8	73.9	30
		Heavy	592.3	956.5	73.9	30
			592.3	478.8	73.9	30
SLC22A3 /OCT3	GPSAAALAE**R**	Light	471.8	630.4	65.5	25.8
			471.8	559.3	65.5	25.8
		Heavy	476.8	640.4	65.5	25.8
			476.8	569.3	65.5	25.8
SLC22A4 /OCTN1	AFILDLF**R**	Light	497.8	663.4	67.4	26.8
			497.8	550.3	67.4	26.8
		Heavy	502.8	673.4	67.4	26.8
			502.8	560.3	67.4	26.8
SLC22A5 /OCTN2	LGSILSPYFVYLGAYD**R**	Light	967.5	1363.7	101.6	43.7
			967.5	571.3	101.6	43.7
		Heavy	972.5	1373.7	101.6	43.7
			972.5	571.3	101.6	43.7
	WLISQG**R**	Light	430.2	673.4	62.5	24.3
			430.2	560.3	62.5	24.3
		Heavy	435.2	683.4	62.5	24.3
			435.2	570.3	62.5	24.3
SLC5A2 /SGLT2	GTVGGYFLAG**R**	Light	549.3	840.4	71.2	28.6
			549.3	563.3	71.2	28.6
		Heavy	554.3	850.4	71.2	28.6
			554.3	573.3	71.2	28.6
ABCG2 / BCRP	ENLQFSAAL**R**	Light	574.8	792.4	73	29.6
			574.8	664.4	73	29.6
		Heavy	579.8	802.4	73	29.6
			579.8	674.4	73	29.6
	LFDSLTLLASG**K**	Light	632.9	1004.6	77.3	31.6
			632.9	689.4	77.3	31.6
		Heavy	636.9	1012.6	77.3	31.6
			636.9	697.4	77.3	31.6

SLCO4C1 / OATP4C1	HLPGTAEIQAG**K**	Light	407.9	716.4	60.9	19.8
			407.9	645.4	60.9	19.8
			407.9	577.3	60.9	19.8
		Heavy	410.6	724.4	60.9	19.8
			410.6	653.4	60.9	19.8
			410.6	577.3	60.9	19.8
ATP1A1 /Na+K+ATPase	IVEIPFNSTN**K**	Light	631.3	1049.5	77.1	31.6
			631.3	807.4	77.1	31.6
		Heavy	635.4	1057.5	77.1	31.6
			635.4	815.4	77.1	31.6
	YHTEIVFA**R**	Light	568.3	835.5	72.5	29.3
			568.3	734.4	72.5	29.3
			568.3	605.4	72.5	29.3
		Heavy	573.3	845.5	72.5	29.3
			573.3	744.4	72.5	29.3
			573.3	615.4	72.5	29.3

Supplemental Table 4: Abundance of kidney transporters across species.

Transporters	Protein abundance (pmol/gram kidney)				
	Human	Monkey	DOG	Rat	Mouse
SLC22A6 /OAT1	107.7 ± 56.83	242.5 ± 62.69	75.4 ± 43.07	308.8 ± 79.24	156.2 ± 92.06
SLC22A7 /OAT2	19.8 ± 8.36	27.3 ± 10.2	NC	BLQ	120.3 ± 39.3
SLC22A8 /OAT3	78.5 ± 37.38	124.7 ± 32.57	NC	NC	NC
SLC22A11 /OAT4	10.6 ± 5.64	17.5 ± 6.28	NC	NC	NC
SLCO4C1 /OATP4C1*	0.3 ± 0.03	0.7 ± 0.28	NC	NC	NC
SLC22A1 /OCT1*	BLQ	BLQ	NC	38.3 ± 6.45	18 ± 3.96
SLC22A2 /OCT2	164.2 ± 53.27	464.8 ± 147.18	NC	253.5 ± 70.92	429.1 ± 134.67
SLC22A3 /OCT3*	0.03 ± 0.01	BLQ	BLQ	NC	NC
SLC22A4 /OCTN1	27.2 ± 13.44	19 ± 10.55	NC	NC	NC
SLC22A5 /OCTN2	13.1 ± 5.8	45 ± 14.35	16 ± 5.84	96.6 ± 22.51	41.4 ± 9.29
ABCB1 /MDR1	42.3 ± 16.16	52 ± 9.44	32.1 ± 9.34	39.3 ± 11.76	15.5 ± 5.99
SLC47A1 /MATE1	105.6 ± 47.52	161.2 ± 56.23	NC	NC	NC
ABCG2 /BCRP*	NC	NC	NC	1.3 ± 0.4	3.1 ± 0.88
ABCC1 /MRP1*	20.1 ± 4.54	54.7 ± 15.7	42.2 ± 10.95	58.3 ± 11.41	50 ± 9.68
ABCC2 /MRP2	30.1 ± 16.52	56 ± 13.99	NC	NC	NC
ABCC3 /MRP3*	20.1 ± 1.78	27.7 ± 9.01	NC	108.7 ± 12.66	29.4 ± 18.42
ABCC4 /MRP4	19.5 ± 20.58	71.3 ± 18.73	NC	37.5 ± 7.51	8.6 ± 3.94
SLC5A2 /SGLT2/	76.4 ± 41.25	182 ± 49.56	356.7 ± 84.85	395.1 ± 67.87	391.7 ± 89.62
ATP1A1 /Na+K+ATPase*	20.1 ± 1.17	51.7 ± 10.91	70.7 ± 15.19	119 ± 14.63	114.9 ± 17.87

*data is presented in relative protein abundance (arbitrary unit)/gram kidney. NC = not conserved peptide, BLQ = Below limit of quantitation

Matrix approach					
	Species				
	S1	S2	S3	S4	S5
Peptides	P1	P1	P1		
			P2		P2
			P3	P3	

Supplemental Figure 1: A schematic representation of matrix approach for estimating the relative abundance of non-conserved peptides. In this example, S1-S5 are the species and P1 –P3 are the peptides. No peptide is conserved across all five species. P1 is conserved in three species (S1 – S3) whereas P2 and P3 are only conserved in two species. The relative abundance (RA) of P1 is estimated using matrix approach by following formula ($RA_{P1S4} = RA_{P3S4} * RA_{P1S3}/ RA_{P3S3}$) Where, RA_{P1S4}, is the estimated relative abundance of P1 in S4, P3. $RA_{P3S4,}$ RA_{P1S3}, and RA_{P3S3} are the measured abundances of P3 in S4, P1 in S3, and P3 in S3, respectively.

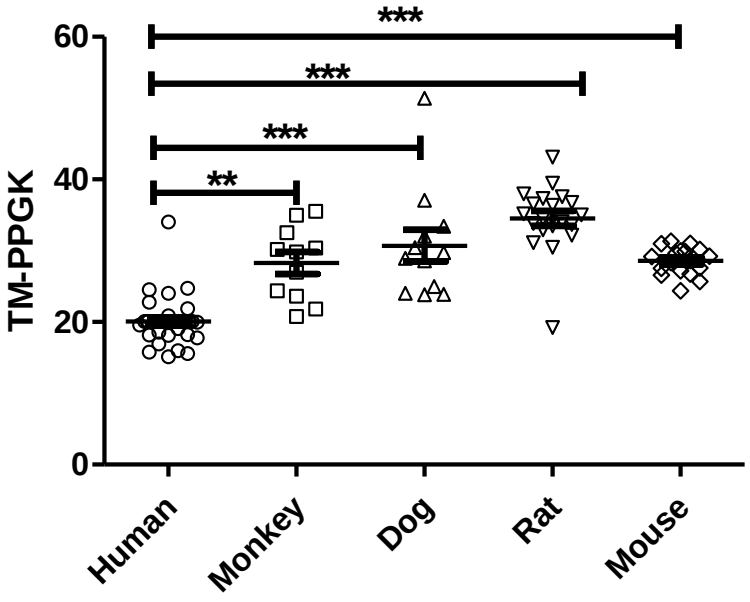

Supplemental Figure 2: Milligram of total membrane protein per gram of kidney (TM-PPGK) across species. Dots indicate individual samples and horizontal line and error bars indicate mean and SD, respectively. The mean TM-PPGK content ± SD was 20.1 ± 3.4 for human (n=34), 28.3 ± 5.1 for monkey (n=11), 30.7 ± 7.7 for dog (n=12), 34.5 ± 4.7 for rat (n=20), and 28.6 ± 2.0 for mouse (n=18).

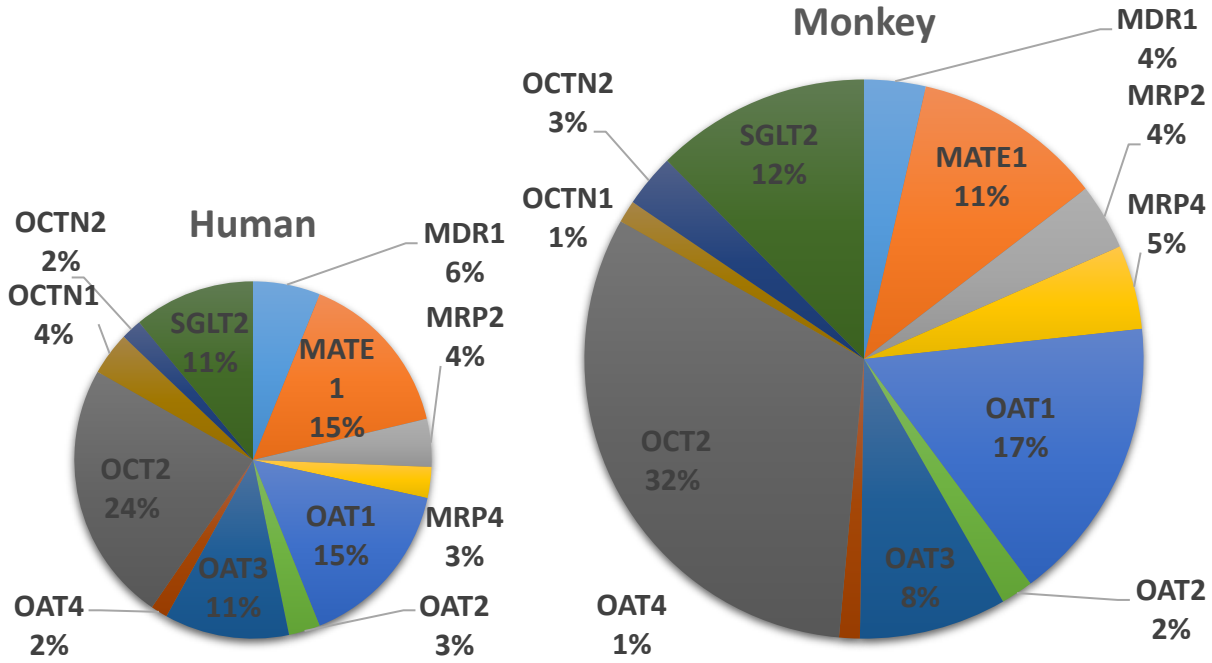

Supplemental Figure 3: Kidney transporters across human and monkey.

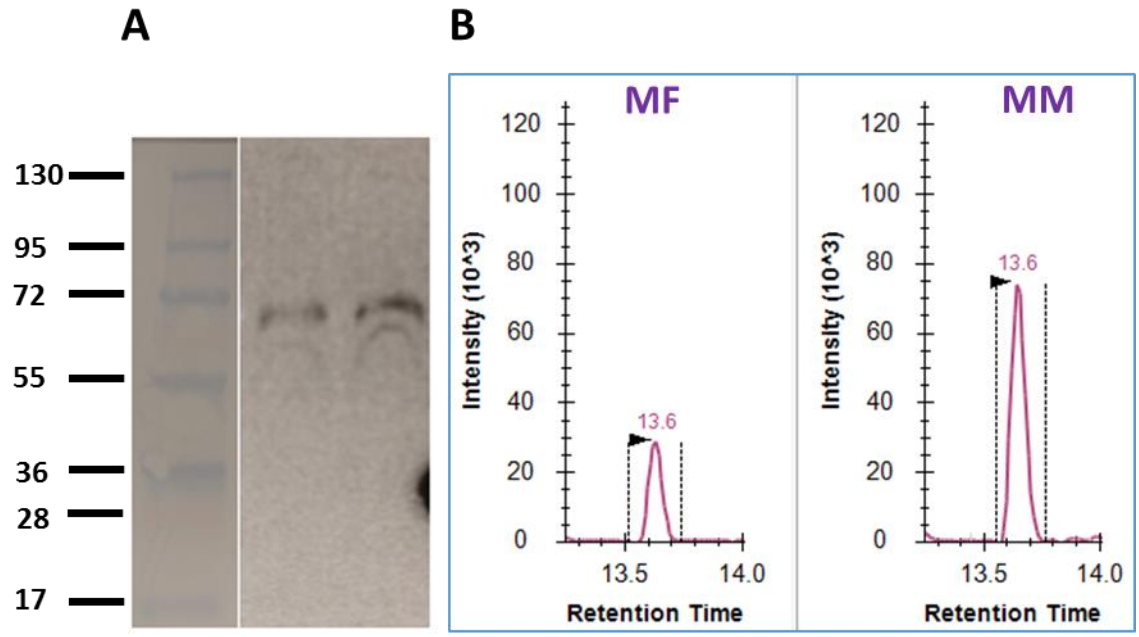

Supplemental Figure 4: Comparison of OAT1 abundance data in representative samples [MF= Mouse (Female); MM = Mouse (Male)] using Western blotting (A) and LC-MS/MS proteomics (B). The band (A) and peak (B) intensities represent relative levels of OAT1 in different samples. In general, the quality of proteomics data is significantly better than the Western blotting data. Western blotting data were generated using a rabbit anti-mouse OAT1 antibody. The sex-difference in OAT1 abundance in mouse is qualitatively confirmed by these results. Although the antibody did not work for human OAT1 (likely because of non-specific binding), the higher rat signal is consistent with the proteomics data (data not shown). The peaks in Figure B represent LC-MS/MS responses of a conserved OAT1 surrogate peptide, GQASAMELLR [m/z 538.28 (++) → 819.43(+)]. Panel A (left) represents the molecular weight markers from nitrocellulose membrane while panel A (right) represents the OAT1 bands from developed X-ray film.

References

Neradugomma NK, Liao MZ, and Mao Q (2017) Buprenorphine, Norbuprenorphine, R-Methadone, and S-Methadone Upregulate BCRP/ABCG2 Expression by Activating Aryl Hydrocarbon Receptor in Human Placental Trophoblasts. *Mol Pharmacol* **91:**237-249.